

Magnetic Simulation of the Hall D Spectrometer - Erratum

M. Lu and G.S. Adams

10 October 2000

This report corrects an error in the previous version of our magnet simulation report (05.06.2000) and shows the results for several modifications of the original LASS magnet geometry. In the previous report an error in the setup of the simulation code resulted in fringe fields that were too large.

A new 2D simulation of the Hall D spectrometer, including the LGD region, has been made. The purpose of the calculation was to obtain estimates of the fringe fields in the regions where detectors will be located. More precise 3D estimates will be carried out by P. Brindza as the spectrometer design evolves.

The calculation was carried out with the Flux2D code. An axially symmetric model of the spectrometer was constructed from Eric Scott's CAD drawing of 15 April. That drawing also forms the basis for the present monte carlo database. We take the coordinate system from that drawing also; the origin is located at the upstream edge of the steel endcap and the z axis is along the beam direction. Zero-field boundary conditions were set at $z = -30\text{m}$, $z = +40\text{m}$, and $r = 40\text{m}$. The materials used in the simulation were either 1010 steel or vacuum. The saturation properties of 1010 steel were interpolated by the code between an initial relative permeability of 3000 and a saturation field of 2.2 Tesla.

Four different geometries are shown here for comparison. In all cases the current was adjusted to produce a central field of 2.2 T. In the first case, the endcap was moved upstream to allow for cable access, but otherwise the magnet has the original LASS configuration (Fig.1). Field maps for this geometry are given in Table 1, and the field lines are shown in Fig.1. For the purposes of comparison one can approximate the radial positions of the Cherenkov and TOF photomultiplier tubes as 132 in and 54 in, respectively. A total of 6.4k grid elements were used in the calculation, and a driving current of 7.0 MA was used. As one can see from Table 1, the fringe fields in the Cherenkov and TOF regions are about 370 gauss and 990 gauss, respectively. While we have no solid numbers from LASS to compare with these, they are commensurate with the heavy magnetic shielding that was needed in that design. Lastly, the field in the region of LGD pmt shields is about 500 gauss, much to high for passive shielding on each tube to be effective without introducing large dead regions in the detector volume.

Table 1:

d (in)	B_{axis} (Tesla) ($r=0.1\text{in}$, $z=40\text{in}+d$)	B_{cerencov}(Tesla) ($z=212\text{in}$, $r=d$)	B_{tof}(Tesla) ($z=228\text{in}$, $r=d$)	B_{lgd}(Tesla) ($z=263\text{in}$, $r=d$)
0.0	2.18	0.31	0.14	0.043
6.0	2.09	0.17	0.10	0.054
12.0	2.12	0.17	0.11	0.050
18.0	2.11	0.16	0.10	0.051
24.0	2.10	0.15	0.098	0.050
30.0	2.09	0.13	0.095	0.049
36.0	2.05	0.12	0.089	0.047
42.0	2.21	0.11	0.086	0.046
48.0	2.12	0.10	0.081	0.044
54.0	2.017	0.099	0.078	0.043
60.0	2.24	0.097	0.075	0.041
66.0	2.20	0.096	0.072	0.040

Table 1:

72.0	2.23	0.093	0.069	0.038
78.0	2.23	0.089	0.065	0.036
84.0	2.28	0.083	0.062	0.034
90.0	2.32	0.076	0.058	0.033
96.0	2.11	0.069	0.053	0.031
102.0	2.23	0.062	0.049	0.029
108.0	2.13	0.057	0.045	0.028
114.0	2.12	0.051	0.041	0.027
120.0	2.17	0.045	0.038	0.025
126.0	1.63	0.041	0.035	0.024
132.0	2.13	0.037	0.032	0.022
138.0	0.49	0.033	0.029	0.021

The need to reduce the fringe field below the values seen in LASS was already recognized in the early versions of our spectrometer design. The easiest way to reduce the fringe field is to fill the existing gaps in the steel yoke with more steel. These gaps will not be needed in our design. In our second case study these gaps were filled, and the driving current reduced to 6.8 MA to maintain the central field at 2.2 T. The results are shown in Fig. 2 and Table 2. This single modification produces a marked reduction in the fringe fields. The fields in the region of the Cherenkov and TOF detectors drop to 77 gauss and 250 gauss, respectively. The field in the region of the LGD is also reduced, but the resulting field of about 200 gauss is still rather high. It is not possible to predict the response of the individual LGD photomultiplier shields using the present 2D model because the LGD lacks the required axial symmetry.

Table 2:

d (in)	B_{axis} (Tesla) (r=0.1in, z=40in+d)	B_{cerencov}(Tesla) (z=212in, r=d)	B_{tof}(Tesla) (z=228in, r=d)	B_{lgd}(Tesla) (z=263in, r=d)
0.0	2.07	0.12	0.049	0.020
6.0	2.10	0.12	0.059	0.019
12.0	2.12	0.11	0.057	0.020
18.0	2.11	0.11	0.053	0.018
24.0	2.11	0.092	0.049	0.018
30.0	2.12	0.078	0.044	0.017
36.0	2.13	0.064	0.038	0.016
42.0	2.18	0.051	0.033	0.015
48.0	2.07	0.040	0.029	0.014
54.0	2.15	0.032	0.025	0.013
60.0	2.30	0.026	0.022	0.013
66.0	2.26	0.022	0.019	0.012
72.0	2.27	0.019	0.017	0.011
78.0	2.30	0.018	0.015	0.010
84.0	2.31	0.016	0.013	0.0093
90.0	2.30	0.015	0.013	0.0087
96.0	2.25	0.013	0.012	0.0081
102.0	2.12	0.012	0.011	0.0075
108.0	2.82	0.011	0.010	0.0070

Table 2:

114.0	3.10	0.010	0.089	0.0065
120.0	2.23	0.0092	0.082	0.0061
126.0	1.91	0.0084	0.0075	0.0057
132.0	1.54	0.0077	0.0070	0.0054
138.0	1.25	0.0071	0.0064	0.0050

Case 3 (Fig. 3 and Table 3) and Case 4 (Fig. 4 and Table 4) add a thin steel cylindrical shell around the LGD region to shield the individual shields that will be used on each photomultiplier. The shell thickness was arbitrarily set to 0.2 in, and the radius was set to 40 in. The cross sectional area of this shell is approximately equal to the area of the LGD. Case 3 adds this shield to the unmodified yoke geometry of Case 1. Case 4 adds this shield to the geometry having the gaps in the yoke filled. Case 4 represents our final result. A grid of 26k elements was used in the calculation and a driving current of 6.8 MA was used. In this case the yoke saturates in a small volume near the downstream bore hole but in the bulk of the yoke the field stays below 2.1 T. The field in the LGD shield goes into saturation in some regions so a thicker box would yield a lower internal field. However it is not clear yet if this is necessary. From Table 4 and Fig. 4 we observe that the fringe field in the regions of the Cherenkov, TOF and LGD detectors is predicted to be about 73 gauss, 220 gauss, and 110 gauss, respectively. These values fall within the range that can be effectively handled with passive shields.

The TOF detectors reside just upstream of the LGD shield. Because of their close proximity to large amounts of magnetic material they will experience a large B field which is hard to calculate accurately, both in magnitude and direction. To use passive shields one must pay careful attention to the direction of the field, and the mechanical stresses can be large. A safer approach may be to design the TOF counters with pmts that can withstand high magnetic fields. Published measurements have shown that good timing resolution can be achieved in this way.

In summary, by filling the gaps in the LASS magnet yoke and adding a passive shield around the LGD detector it is possible to dramatically reduce the expected fringe field in the regions where the Cherenkov, TOF, and LGD photomultipliers will be located. The expected fringe fields are sufficiently small that they can be effectively shielded by individual passive shields around each pmt.

Table 3:

d (in)	B_{axis} (Tesla) (r=0.1in, z=40in+d)	$B_{cerencov}$(Tesla) (z=212in, r=d)	B_{tof}(Tesla) (z=228in, r=d)	B_{lgd}(Tesla) (z=263in, r=d)
0.0	2.10	0.18	0.13	0.039
6.0	2.12	0.18	0.13	0.039
12.0	2.10	0.17	0.12	0.039
18.0	2.07	0.16	0.11	0.039
24.0	2.07	0.15	0.10	0.040
30.0	2.09	0.13	0.096	0.041
36.0	2.12	0.12	0.090	0.042
42.0	2.18	0.11	0.084	2.22
48.0	2.17	0.10	0.079	0.043
54.0	2.17	0.098	0.076	0.042
60.0	2.18	0.096	0.073	0.041
66.0	2.18	0.094	0.070	0.040
72.0	2.22	0.091	0.067	0.039

Table 3:

78.0	2.23	0.087	0.064	0.037
84.0	2.23	0.081	0.061	0.035
90.0	2.21	0.076	0.057	0.034
96.0	2.12	0.069	0.053	0.032
102.0	2.05	0.062	0.049	0.030
108.0	2.23	0.056	0.048	0.029
114.0	1.83	0.050	0.041	0.027
120.0	1.54	0.045	0.038	0.025
126.0	1.11	0.040	0.034	0.024
132.0	0.72	0.036	0.031	0.022
138.0	0.71	0.033	0.029	0.021

Table 4:

d (in)	B_{axis} (Tesla) (r=0.1in, z=40in+d)	B_{cerencov}(Tesla) (z=212in, r=d)	B_{tof}(Tesla) (z=228in, r=d)	B_{igd}(Tesla) (z=263in, r=d)
0.0	2.07	0.14	0.075	0.011
6.0	2.09	0.13	0.072	0.011
12.0	2.07	0.12	0.067	0.011
18.0	2.07	0.11	0.060	0.010
24.0	2.07	0.093	0.052	0.0096
30.0	2.05	0.077	0.044	0.0087
36.0	2.11	0.062	0.037	0.0084
42.0	2.14	0.049	0.030	2.09
48.0	2.17	0.038	0.025	0.011
54.0	2.23	0.030	0.022	0.012
60.0	2.23	0.024	0.019	0.011
66.0	2.23	0.021	0.017	0.011
72.0	2.27	0.018	0.015	0.010
78.0	2.27	0.016	0.014	0.0095
84.0	2.28	0.015	0.013	0.0088
90.0	2.24	0.014	0.012	0.0083
96.0	2.27	0.012	0.011	0.0077
102.0	2.06	0.011	0.0098	0.0072
108.0	2.19	0.010	0.0091	0.0067
114.0	1.89	0.0094	0.0084	0.0063
120.0	1.82	0.0086	0.0077	0.0059
126.0	0.99	0.0079	0.0071	0.0055
132.0	0.96	0.0073	0.0066	0.0052
138.0	0.73	0.0067	0.0061	0.0048

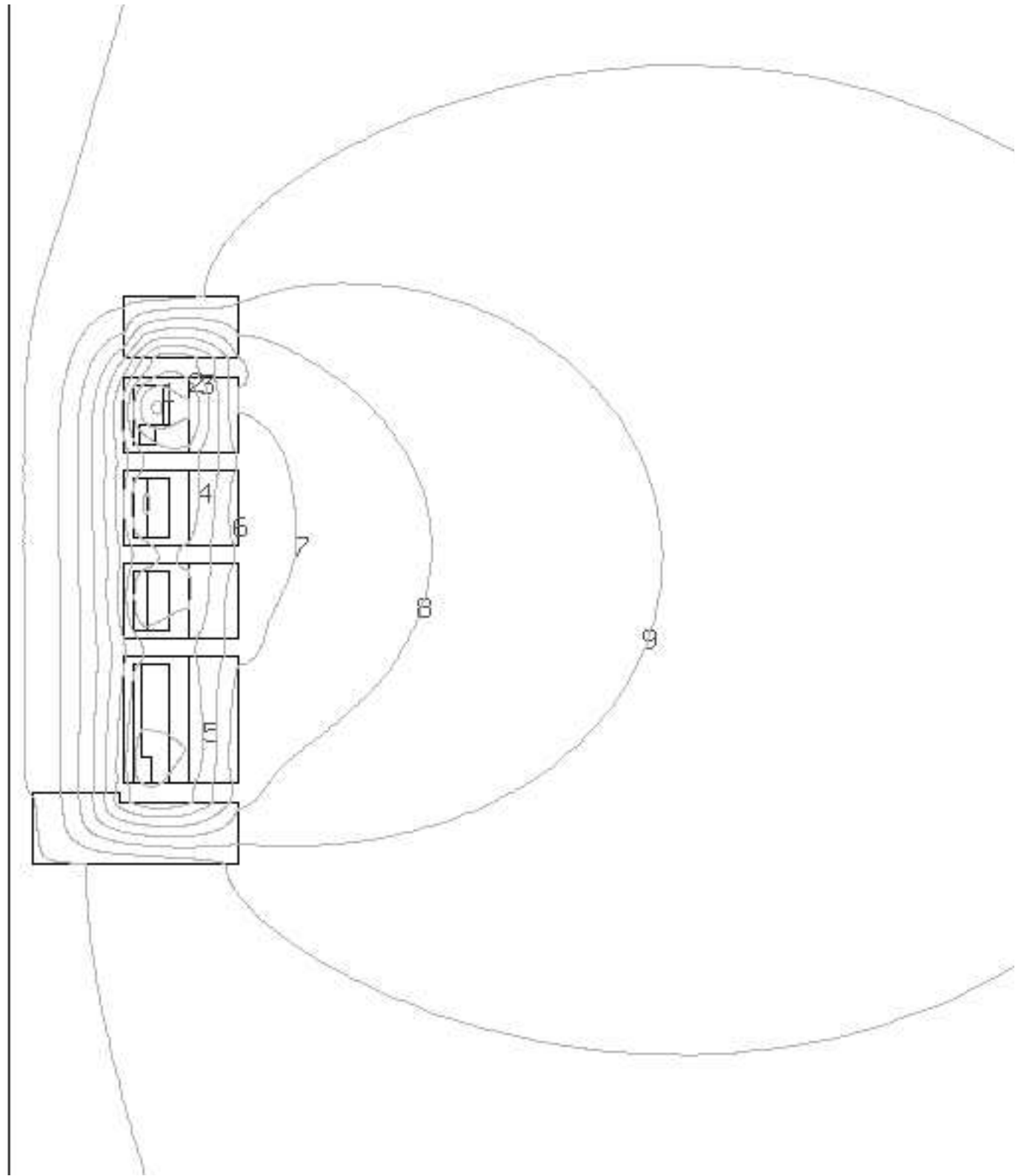


Fig. 1 - Case 1 geometry and field.

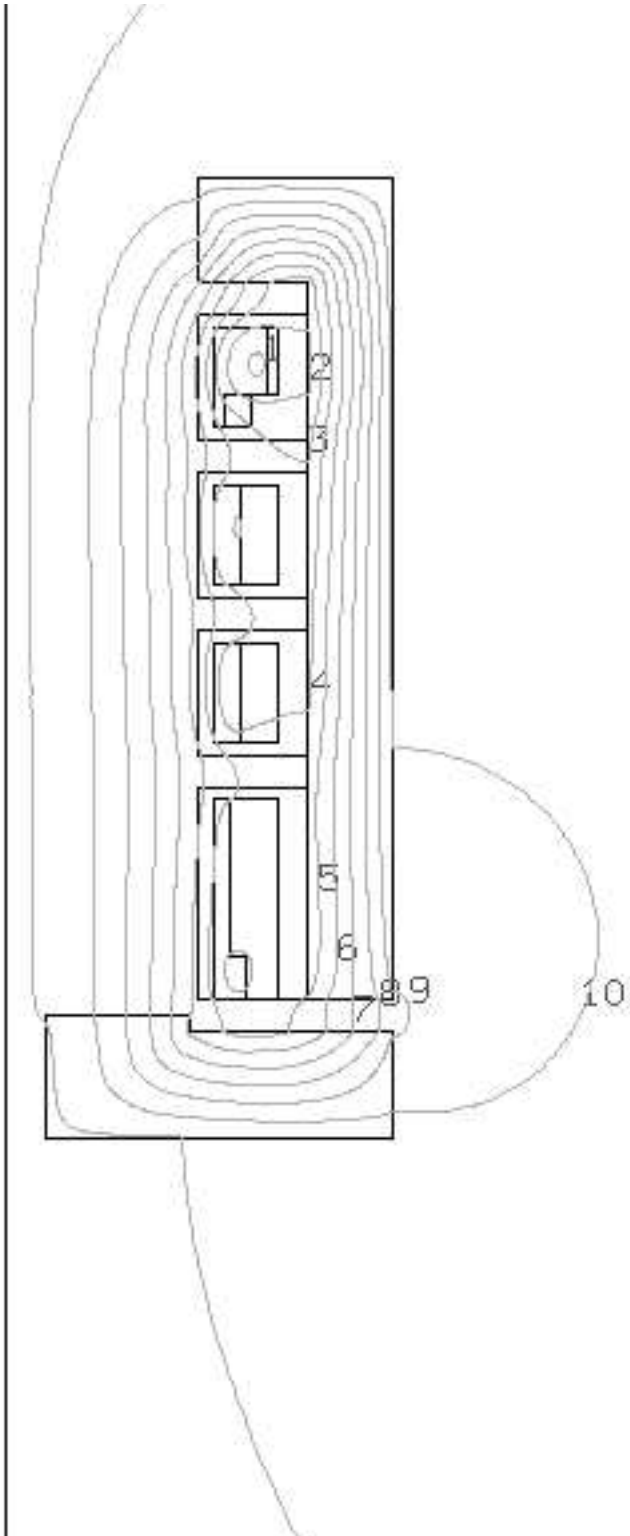


Fig. 2 - Case 2 geometry and field.

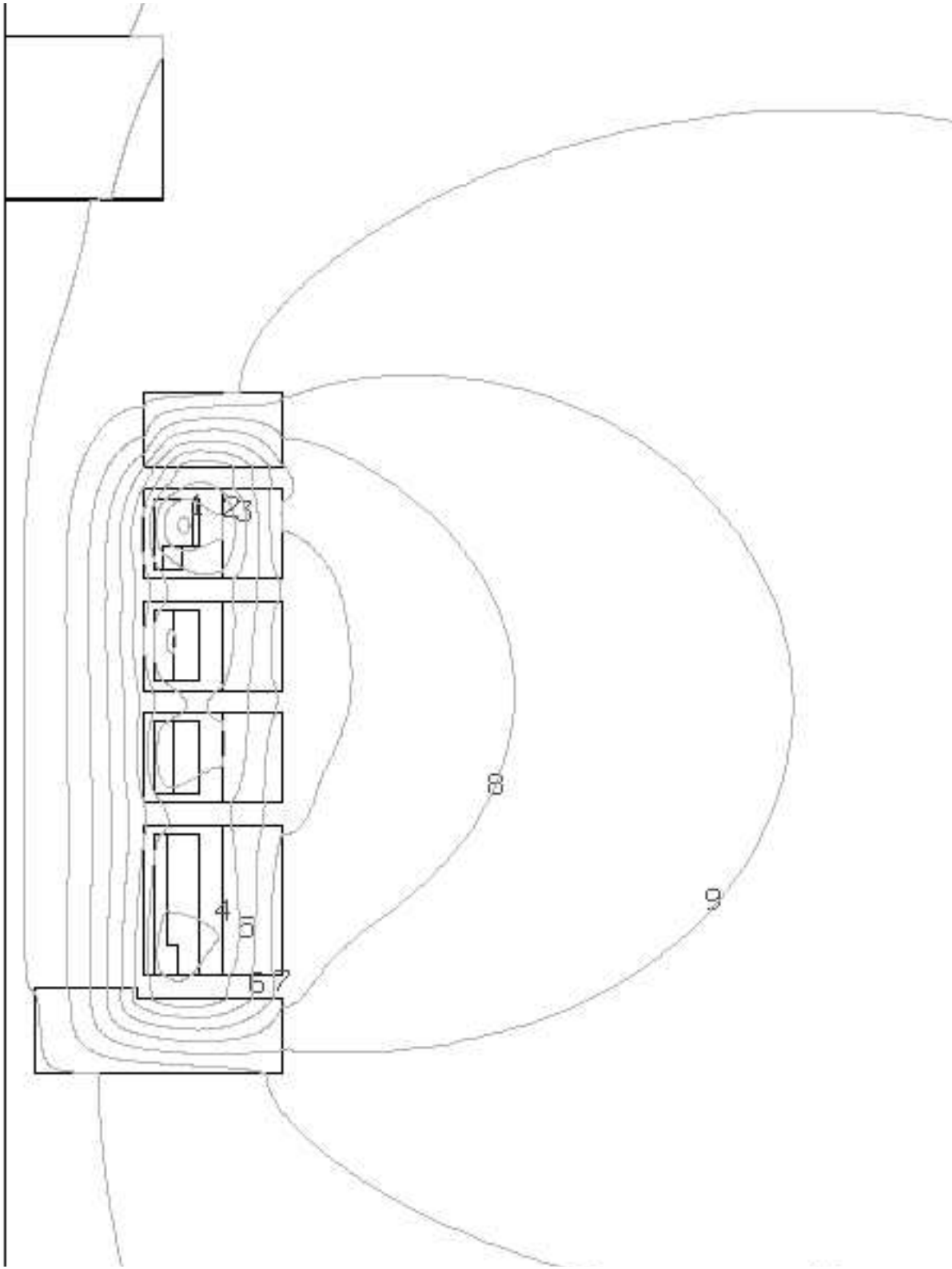


Fig. 3 - Case 3 geometry and field.

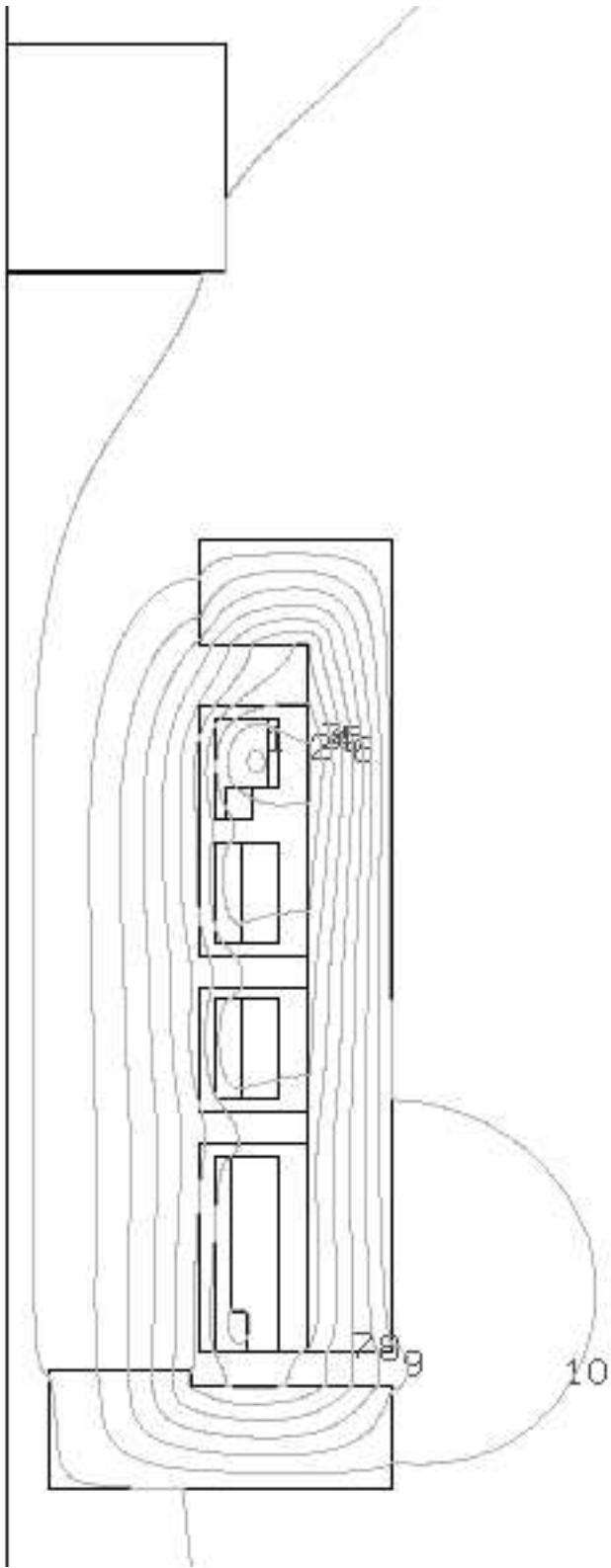


Fig. 4 - Case 4 geometry and field; final result.